

# Modeling of hole generation process in AlGaIn/GaN HEMTs

Ying-Chun Kuo<sup>1,2,✉</sup>, Hao Yu<sup>1,✉</sup>, Nelson de Almeida Braga<sup>3</sup>, Jingtian Fang<sup>3</sup>, Amratansh Gupta<sup>1,2</sup>, Sachin Yadav<sup>1</sup>, AliReza Alian<sup>1</sup>, Uthayasankaran Peralagu<sup>1</sup>, Nadine Collaert<sup>1,2</sup>, Bertrand Parvais<sup>1,2</sup>

<sup>1</sup>imec, Leuven, Belgium, <sup>2</sup>Vrije Universiteit Brussel, Brussels, Belgium, <sup>3</sup>Synopsys, California, USA

✉ Email: ying-chun.kuo@imec.be; hao.yu@imec.be

**Abstract**—The process of hole generation in GaN HEMTs during the semi-on state continues to be an active field of research. This study analyzes the  $V_{DS}$  dependence of hole current in AlGaIn/GaN HEMTs using an extended Okuto-Crowell model that accounts for both low-field onset and high-field saturation effects. The model accurately explains the non-conventional bias dependence of the measured hole current. This model enables the simulation of trap-assisted hole generation and may serve as a foundation for future TCAD studies of related phenomena, such as threshold voltage instability and the kink effect.

**Index Terms**—AlGaIn/GaN HEMT, semi-on state, hole current, hot carrier induced hole generation, TCAD modeling

## I. INTRODUCTION

Gallium Nitride (GaN)-based high-electron-mobility transistors (HEMTs) are ideal for RF switches and power amplifiers due to their high channel conductivity and high breakdown voltage [1]. RF GaN power amplifiers (PAs) typically operate in deep-class AB, requiring devices to maintain robustness across various operating states, including off, semi-on, and fully-on states. The deep class-AB PA is quiescently biased in the semi-on state (gate bias slightly above threshold voltage, drain bias at supply voltage), making the robustness in the semi-on state particularly critical. The semi-on state is accompanied by hot electron effects, due to the concurrent high current density and high electric field at the gate-drain corner in the channel. Hole generation induced by hot carriers (Fig. 1) is one of the reliability concerns and can lead to reliability issues such as threshold voltage shifts and kink effects in the transfer or output characteristics of (MIS)HEMTs [2], [3]. However, the underlying physics of the hole generation process in a GaN HEMT is still under debate. Some studies assume that holes are generated by impact ionization [2]–[4], but experimental evidence against impact ionization has also been reported [5], [6]. In this study, we investigate the  $V_{DS}$  dependency of the hole current collected at the gate, which differs from that of the impact ionization process. We developed a hole generation model in Sentaurus TCAD [7] to capture experimental observations.

## II. EXPERIMENTAL

The hole current was all measured on GaN-on-Si HEMTs. The III-nitride stacks are illustrated in Fig. 1. The epitaxial

stack was grown by MOCVD on a 200nm high resistivity Si substrate, followed by an  $\text{Al}_x\text{Ga}_{1-x}\text{N}$  superlattice buffer. Above this, the III-N stacks include a carbon-doped GaN back barrier, a 100-nm unintentionally doped GaN channel, and a 1 nm AlN interlayer to reduce alloy scattering. This is followed by a 15nm AlGaIn top barrier with a 7-nm recess, and a 5nm *in-situ* SiN<sub>x</sub> for surface passivation. Finally, a 5 nm Al<sub>2</sub>O<sub>3</sub> layer and a 140 nm SiO<sub>2</sub> layer were deposited as the gate dielectric and passivation stack. More details of fabrication can be found in Ref. [8]. The devices under test in this research are all with a gate width of 10  $\mu\text{m}$ ,  $L_g = 0.13 \mu\text{m}$ ,  $L_{gs} = 1.5 \mu\text{m}$ ,  $L_{gd} = 1.75 \mu\text{m}$ .

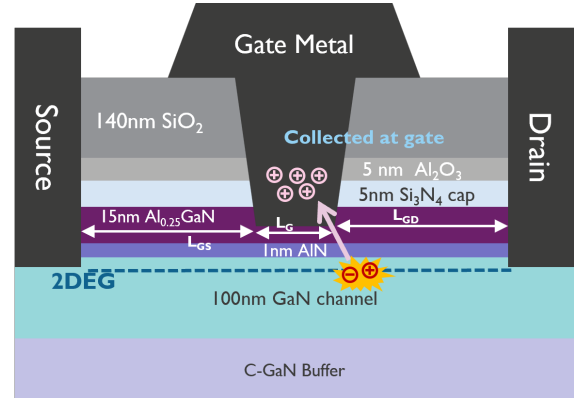


Fig. 1: Cross-sectional schematic of the HEMT under study, illustrating the generation of holes at the gate-drain (GD) corner in the channel; a fraction of these holes is collected at the gate terminal as the hole current component  $I_{G,h}$ .

## III. HOLE CURRENT EXTRACTION

DC  $I_G - V_G$  sweeps were performed at  $V_{DS} = 5\text{V}$  to 20V in 2.5V steps with the source grounded all at room temperature. The  $I_G - V_G$  curve contains a bell-shaped hole current ( $I_{G,h}$ ) and a background gate leakage current ( $I_{G,leakage}$ ), i.e.,  $I_G \approx I_{G,h} + I_{G,leakage}$ , which is the typical characteristic of the hole generation in the semi-on state. Under source-floating conditions, although a high electric field still exists at the gate-drain (GD) corner, the absence of current flow in the channel means no hot carriers are generated. Consequently,

$I_{G,h}$  is not observed in experiments (Fig. 2), confirming that hole generation is induced by hot carriers from conductive  $I_{DS}$ .

Since hole generation is induced by hot carriers and strongly dependent on the electric field, the characteristic bell-shaped  $I_{G,h}$  profile along the  $V_G$  sweep can be divided into three regions, as previously reported in [3], [4]: (1) when  $V_{GS} - V_{th} < 0V$ , though a strong electric field present at the GD corner, but the lack of carriers in the channel results in no hole generation. Only reverse gate leakage was observed. (2) when  $0 < V_{GS} - V_{th} < 1V$ , the hole current increases as  $I_D$  rises, providing more hot carriers. (3) when  $V_{GS} - V_{th} > 1V$ , the hole current decreases due to a reduction in the electric field as  $V_G$  increases.

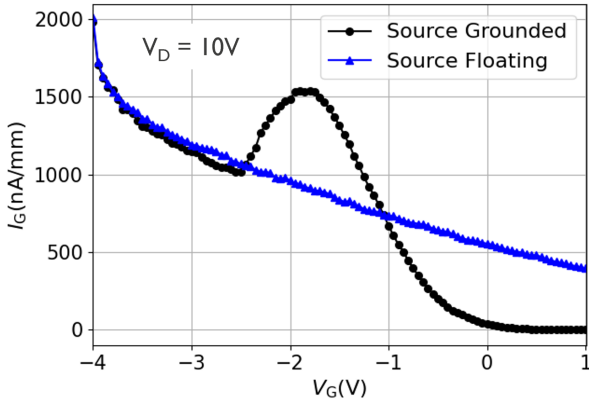


Fig. 2: Measured HEMT gate current as a function of gate voltage at  $V_D = 10$  V. The hole current bump is not observed with a floating source terminal, suggesting that the generation of holes is induced by hot carriers.

In HEMT measurements, the gate leakage is comparable to the hole current collected at the gate, making it essential to extract the hole component from the total gate current. To do this, we numerically identified the start and end points of the  $I_G$  bump and applied a linear fit to represent the background leakage current  $I_{G,leakage}$ . By subtracting this fitted leakage from the total gate current, we obtained the pure hole current  $I_{G,h}$ , shown as the blue line in Fig. 3. The peak value of the hole current bump  $I_{G,h}$  is then extracted to represent the magnitude of hole generation in the channel and analyze its dependence on  $V_{DS}$ , enabling the study of the underlying physical mechanism.

The extracted peak values of  $I_{G,h}$  are shown in Fig. 4. The measurement data, shown in black, exhibit an initial increase with  $V_{DS}$ , followed by saturation at approximately  $V_{DS} = 10V$ . This  $V_{DS}$  dependency deviates from the impact ionization behavior, where hole generation is expected to increase continuously with  $V_{DS}$  due to the rising electric field [9]. The blue triangles in Fig. 4 showed the HEMT simulation results using the Okuto-Crowell impact ionization model with parameters from T. Maeda [10], who experimentally extracted the generation coefficient from a GaN p-n diode. This simulation exhibits a larger increase in the peak value of  $I_{G,h}$  at higher  $V_{DS}$ , revealing a clear discrepancy with the

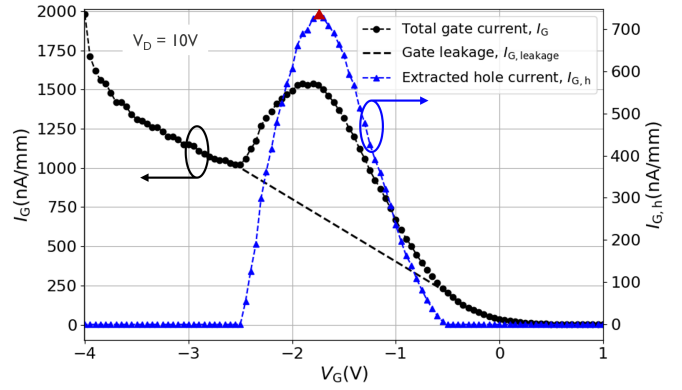


Fig. 3: Extraction of the hole current component (blue with symbols) from the total gate current (black line with symbols) by subtracting the estimated background gate leakage (black dashed line). The peak (red mark) is extracted for  $V_{DS}$  dependence analysis.

experimental data. Additionally, the  $V_{GS}$  dependence shown in Fig. 5 indicates that the  $I_{G,h}$  bump simulated using this model exhibits a much narrower peak region than the measured data. The poor agreement of both  $V_{DS}$  and  $V_{GS}$  dependencies with the impact ionization model and its parameters suggests the presence of a hole generation mechanism other than impact ionization.

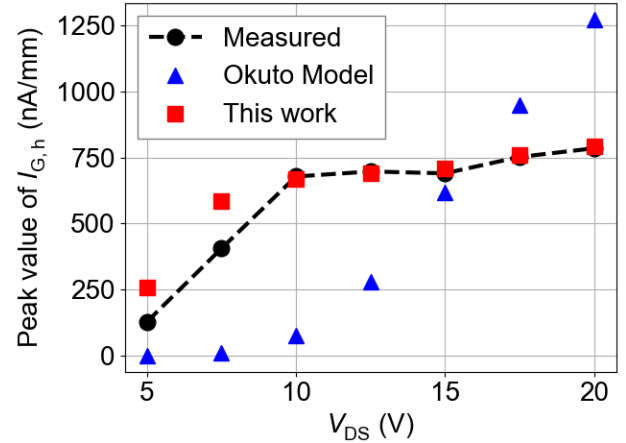


Fig. 4: Peak  $I_{G,h}$  vs.  $V_{DS}$ : comparison of measurement, original model, and proposed model. The proposed model accurately captures the  $V_{DS}$  dependence, showing good agreement with the measurement data.

#### IV. HOLE GENERATION MODELING

Due to the inconsistent behavior between the experimental data and the conventional impact ionization model, we propose a trap-assisted hole generation process, as illustrated in the right plot of Fig. 6. In this model, the limited availability of traps is assumed to constrain the increase in hole generation under high electric fields. To capture this behavior, we introduced an empirical model based on the Okuto-Crowell framework with an additional saturation term, and implement it in TCAD simulations to reproduce the observed hole generation characteristics. This modified

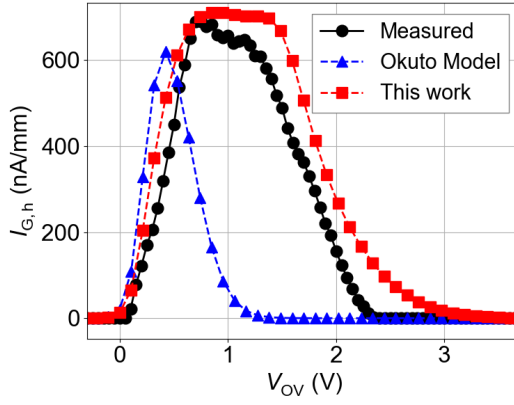


Fig. 5: Comparison of measured  $I_{G,h}$  vs.  $V_{OV}$  with simulations using conventional impact ionization models and the modified hole generation model. The bell-shaped hole currents all begin to rise at zero gate overdrive. The modified model with a lower  $E_0$  results in a wider  $I_{G,h}$  bump width, consistent with the measurement data. Bias conditions:  $V_{DS} = 15V$ ,  $V_{GS}$  swept from  $-4V$  to  $1V$ .

model is implemented in Synopsys Sentaurus<sup>TM</sup> using the Physical Model Interface (PMI). Figure 7 shows the hole generation mapping based on the proposed model, illustrating that generation typically occurs near the corner region, where the electric field is strongest.

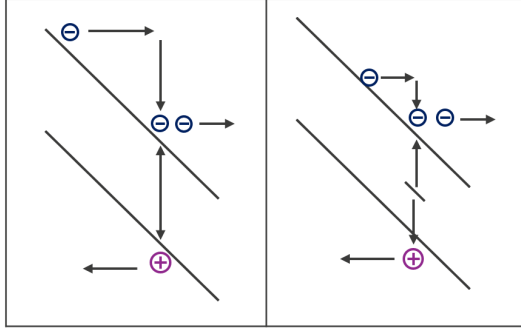


Fig. 6: (Left) Band-to-band impact ionization; (right) Trap-assisted impact ionization which can explain the onset of hole generation at relatively low electric fields.

The trap-assisted generation coefficient is the core of model for hole generation process, which represents the probability that an electron or hole creates an electron-hole pair via the trap-assisted process per unit distance traveled in GaN channel. In this study, the coefficient is redefined as a function of the electric field as:

$$\alpha_{TA}(E) = \alpha_0 \cdot \left( -\frac{E_0}{E} \right) \cdot \frac{1}{1 + \left( \frac{E}{E_{sat}} \right)^n} \quad [cm^{-1}] \quad (1)$$

where  $\alpha_0$ ,  $E_0$ ,  $E_{sat}$  and  $n$  are model parameters representing the hole current peak, the critical electric field, the starting point of saturation, and the degree of saturation, respectively. The redefined generation coefficient  $\alpha_{TA}$  is then incorporated into the well-known expression for the total generation rate,

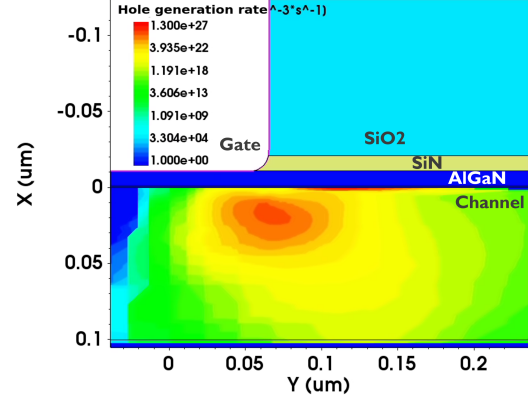


Fig. 7: Mapping of hole generation rate with the modified model at  $V_{DS} = 15V$ ,  $V_G = -3V$  ( $V_{OV} = 0.3V$ ), showing generation at the GD corner.

which quantifies the rate at which electron-hole pairs are generated:

$$G = \alpha_{n,TA} n v_n + \alpha_{p,TA} p v_p \quad [cm^{-3}s^{-1}] \quad (2)$$

In this equation,  $\alpha_{n,TA}$  and  $\alpha_{p,TA}$  are the redefined trap-assisted generation coefficients due to hot electrons and hot holes, respectively,  $n$  and  $p$  are carrier densities, and  $v_n$  and  $v_p$  are carrier velocities. Since hot electrons play a dominant role in the generation process, the contribution from hot holes is typically negligible.

Finally, the hole current is computed as:

$$I_h = q \cdot G \cdot V, \quad I_{G,h} = f_G \cdot I_h \quad [A] \quad (3)$$

where  $G$  ( $cm^{-3}s^{-1}$ ) is the hole generation rate,  $V$  ( $cm^3$ ) is the effective volume where holes are generated,  $q$  is the elementary charge, and  $I_h$  represents the total hole current. The hole current collected at the gate ( $I_{G,h}$ ) is a fraction of the total hole current  $I_h$ . As shown in Fig. 8, only part of the holes generated in the channel reach the gate, with the collection efficiency characterized by  $f_G$ .

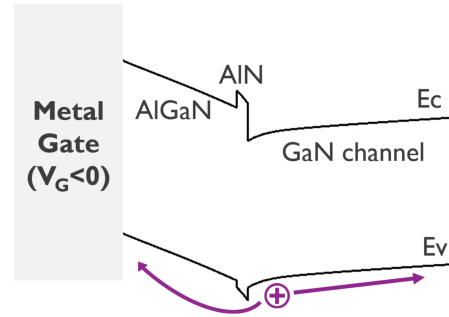


Fig. 8: The band diagram along the vertical cutline in the channel at the semi-on state shows that holes generated in the channel may move either toward the C-GaN layer behind the channel or toward the gate, according to the valence band energy profile.

Using the calibrated parameters listed in Table I, the proposed model successfully reproduces the bias dependence of the hole current collected at the gate  $I_{G,h}$ . Unlike conventional impact ionization models, it captures two key characteristics

observed in the measurements: (i) saturation of  $I_{G,h}$  at high electric fields and (ii) initiation of hole generation at lower  $V_{DS}$  due to a reduced critical electric field  $E_0$ .

As shown in Fig. 4, the model aligns well with the measured peak  $I_{G,h}$ , accurately capturing the saturation behavior. In Fig. 5, it also reproduces the bell-shaped  $I_{G,h}$  versus gate overdrive ( $V_{OV}$ ) curves, where the lower  $E_0$  value broadens the  $V_{OV}$  range for hole generation. These behaviors support the assumption of a trap-assisted mechanism for hole generation: (1) the total number of traps limits the maximum  $I_{G,h}$  under high electric field; and (2) trap assistance lowers the energy required for hot carriers to generate electron-hole pairs.

## V. MODEL CALIBRATION

The hole generation model in this work can be calibrated for a given transistor using the following steps:

- (i) Extract the electric field from TCAD simulations and obtain the experimental  $I_{G,h}$  at a given  $V_G$  and  $V_D$ .
- (ii) Calibrate  $E_0$  to match the  $V_{DS}$  positive dependence of  $I_{G,h}$  in the low- $V_{DS}$  regime;
- (iii) Determine  $E_{sat}$  and  $n$  to capture the saturation behavior at high- $V_{DS}$  regime;
- (iv) Adjust  $\alpha_0$  to align the magnitude of experimental and simulated  $I_{G,h}$ .

Table I lists the calibrated parameters.

	T. Maeda Parameters	This work
$\alpha_0$ (cm <sup>-1</sup> )	2.69e7	8.32e2
$E_0$ (V/cm)	2.27e7	4e6
$E_{sat}$ (V/cm)		1.2e6
$n$		20

TABLE I: Parameter set from Ref. [10] (1st column) and the corresponding values used in this model for  $\alpha_n, \alpha_{TA}$ .

## VI. CONCLUSION

In this study, we experimentally observed a unique hot-carrier-induced hole generation process that cannot be explained by conventional impact ionization models. We developed a trap-assisted model that successfully describes both the high-field saturation and the low-energy trigger behavior of hole generation, as demonstrated by its strong agreement with experimental hole current data versus  $V_{GS}$  and  $V_{DS}$ . The model was calibrated through a systematic process using TCAD-extracted electric fields and experimental data, enabling accurate parameter extraction across different bias regimes. Our modeling reveals that in the semi-on state, the dominant hole generation mechanism in the experimental HEMTs is not direct impact ionization but rather a trap-assisted effective impact ionization process. The model paves the way for further simulations of hole generation-related effects, such as  $V_{th}$  instability and kink effects in  $I_D-V_G/I_D-V_D$  characteristics of GaN (MIS)HEMTs.

## REFERENCES

- [1] Collaert, N., et al. "III-V/III-N technologies for next generation high-capacity wireless communication." *2022 International Electron Devices Meeting (IEDM)*. IEEE, 2022. DOI: 10.1109/IEDM45625.2022.10019555.
- [2] Brar, B., et al. "Impact ionization in high performance AlGaIn/GaN HEMTs." *IEEE Lester Eastman Conference on High Performance Devices*. IEEE, 2002. DOI: 10.1109/LECHPD.2002.1146791.
- [3] Yeh, Yu-Hsuan, et al. "Obtaining impact ionization-induced hole current by electrical measurements in gallium nitride metal-insulator-semiconductor high electron mobility transistors." *Journal of Physics D: Applied Physics* 54.28 (2021): 285104. DOI: 10.1088/1361-6463/abfad5.
- [4] Bisi, Davide, et al. "Observation of hot electron and impact ionization in N-polar GaN MIS-HEMTs." *IEEE Electron Device Letters* 39.7 (2018): 1007–1010. DOI: 10.1109/LED.2018.2835517.
- [5] Dong, Qingyang, et al. "Temperature nonmonotonic behavior of GaN HEMTs kink effect caused by trap-assisted impact ionization." *IEEE Transactions on Electron Devices* 71.3 (2024): 1798–1804. DOI: 10.1109/TED.2024.3354214.
- [6] Zhan, Gao, et al. "Transconductance overshoot, a new trap-related effect in AlGaIn/GaN HEMTs." *IEEE Transactions on Electron Devices* 70.6 (2023): 3005–3010. DOI: 10.1109/TED.2023.3270134.
- [7] Sentaurus Device User Guide, Version U-2022.12.
- [8] Peralagu, Uthayasankaran, et al. "CMOS-compatible GaN-based devices on 200mm-Si for RF applications: Integration and Performance." *2019 IEEE International Electron Devices Meeting (IEDM)*. IEEE, 2019. DOI: 10.1109/IEDM19573.2019.8993582.
- [9] Okuto, Y., and C. R. Crowell. "Threshold energy effect on avalanche breakdown voltage in semiconductor junctions." *Solid-State Electronics* 18.2 (1975): 161–168. DOI: 10.1016/0038-1101(75)90099-4.
- [10] Maeda, Takuya, et al. "Impact ionization coefficients and critical electric field in GaN." *Journal of Applied Physics* 129.18 (2021). DOI: 10.1063/5.0050793.